Effect of Boron Content on Carbon Steel Welds

Study shows how boron affects the microstructure, notched tensile strength and hardenability of carbon steel welds

BY J. H. DEVLETIAN AND R. W. HEINE

ABSTRACT. This investigation provides an experimental analysis of boron's effect on the hardenability, microstructure and notched tensile strength of carbon steel welds which were deposited by the GTA and GMA welding processes. Single pass welds were deposited on ¼ in. thick 1020 and 10B20 steel plates using filler metal of varying boron contents.

Boron was found to significantly affect the microstructure of steel weld metal by effectively retarding the pearlite reaction during weld cooling in favor of the transformation to a bainitic carbide-ferrite aggregate (granular bainite). Furthermore, the amount of $Fe_{23}(B,C)_6$ borocarbide precipitation forming at prior austenite grain boundaries and solidification cell boundaries was found to increase with increasing boron content and decreasing weld cooling rate.

Boron's hardenability effect was found to be just as potent in weld metal as it was in wrought steel of the same composition. The hardenability of as-deposited welds was measured by comparing the weld cooling rate and hardness with similar cooling rates and hardness data from Jominy end quenched bars of the same steel.

Although the notched tensile strength of boron steel welds was superior to boron-free steel welds, boron's strengthening effect was greatly dependent upon the amount of boron present in the weld. In fact, maximum notched tensile strength was attained in 0.2% C steel weld metal with an optimum boron content of 0.002%. The reduction of notched strength at excessive boron concentrations was due to the presence of embrittling intergranular and intercellular borocarbides.

Furthermore, in GTA, GMA and also submerged arc welds notched tensile strength varied directly as a function of the "soluble" boron content rather than the total boron content. Because of the faster weld cooling, GTA and GMA welds were significantly stronger than the slower cooling submerged arc welds.

Introduction

The objective of this investigation was to determine the effect of boron content upon the microstructure, notched tensile properties and hardenability of plain carbon steel weld metal, as deposited by the GTA, GMA and submerged arc welding processes.

Although little is known about boron's behavior in welds, it is well known that minute percentages of boron greatly increase the hardenability of wrought steels. For example, the increased hardenability produced by the addition of only 0.0005 to 0.003% boron to a 0.2% carbon steel is equivalent to that produced by about 0.9% Cr, 3.2% Ni or 0.7% Mo. However, it has also been found that boron's potency is contingent upon (a) carbon content and (b) boron content.

Generally, as the carbon content of a wrought steel increases up to the eutectoid composition, boron's hardenability factor decreases linearly (Refs. 3-6) as illustrated in Fig. 1. Consequently, boron additions appear to be most effective in high alloy, low carbon steels and virtually useless in eutectoid steels.

The boron content has also been found to significantly affect the hardenability of steels (Refs. 1,2,3, and 6). Melloy et al (Ref. 6) have shown that there exists an optimum boron concentration whereby maximum hardenability is attained. For example, boron was found to increase the hardenability of a low carbon, Mo steel (ASTM A514-J) by as much as a factor of 3 for an optimum boron content of 0.0020%.

However, if the boron concentration is excessive, a borocarbide constituent, identified as $Fe_{23}(B,C)_6$, forms at the austenite grain boundaries of wrought steels (Ref. 6). Similarly, it has been demonstrated that this borocarbide also precipitates at cell and dendrite boundaries during cooling of GTA and GMA welds (Ref. 7).

It is precisely this borocarbide constituent that is of prime interest in this investigation. The presence of the intergranular $Fe_{23}(B,C)_6$ constituent was found to not only decrease boron's hardenability effect but also

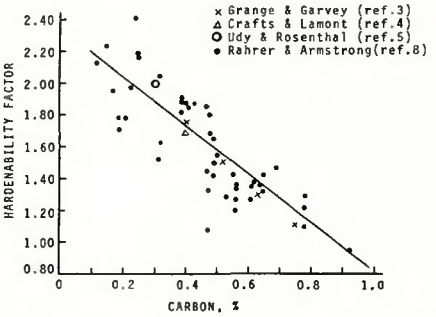

Fig. 1 — Effect of carbon content on boron's hardenability factor in steel

J. H. DEVLETIAN is Assistant Professor of Materials Science, Youngstown State University, Youngstown, Ohio, and R. W. HEINE is Professor of Metallurgical Engineering, University of Wisconsin-Madison, Madison, Wisconsin.

Paper was selected as alternate for the 55th AWS Annual Meeting held at Houston, Texas, during May 6-10, 1974.

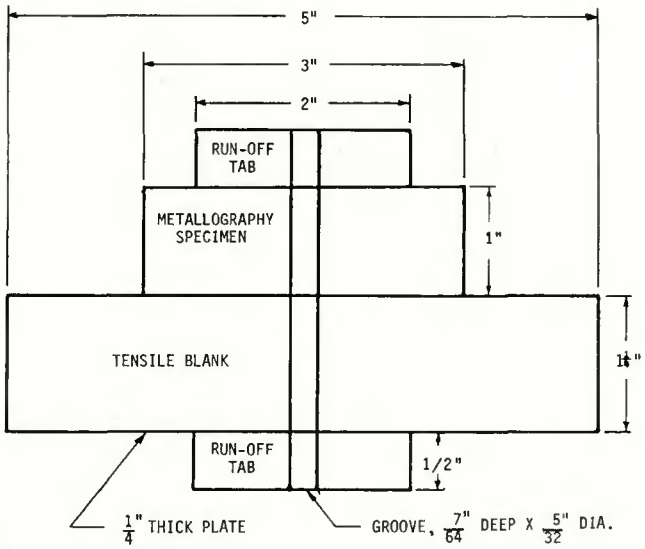

Fig. 2 — Workpiece preparation prior to GTA, GMA and submerged arc welding

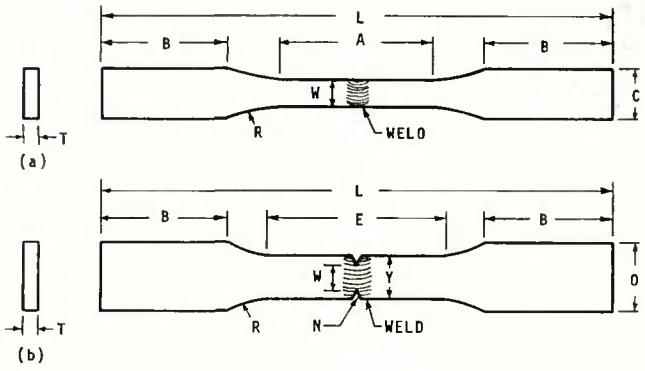

DIMENSIONS

L - 5 in.
C - 0.500 ± .015 in.
D - 0.600 ± .015 in.
W - 0.250 ± .005 in.
B - 1 in. min.
Y - 0.375 ±.005 in.
R - 1 in. min.
T - 0.120 ± .005 in.
A - 1.24 in.
E - 1.50 in.
N - Notch: 60° ± 5° with 0.003 ± .005 in. radius

Fig. 3 — Flat tensile specimens (a) unnotched and (b) notched at the weld

Table 1 — Chemical Compositions of Steel Plate and Filler Metal

Steel	C	B	Mn	Al	Si	Remarks[a]
1020	.19	—	.50	.005	.20	1
10B20	.19	.0017	.71	.08	.22	1
10B20E	.19	.003	.71	.08	.22	2
10B20F	.19	.0042	.71	.08	.22	2
B-3	.19	.0082	.71	.08	.22	2
B-4	.19	.024	.70	.08	.22	2

(a) 1 = commercial steel; 2 = melted 10B20 steel and added alloying elements under dry argon atmosphere

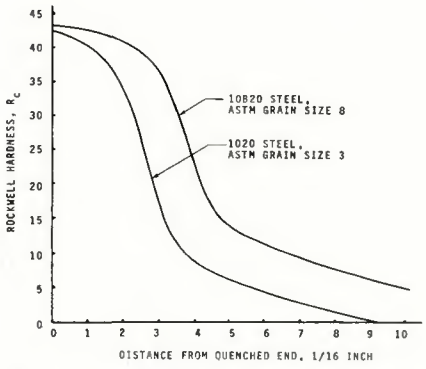

Fig. 4 — Jominy end quench test for 1020 and 10B20 steel, austenitized at 1700 F — 1 hour

seriously affect the notched toughness of steel. For example, when boron contents exceeded a value of 0.0025% in a low carbon steel, both hardenability and toughness deteriorated due to the formation of this embrittling borocarbide precipitate (Ref. 6).

Experimental Procedure

Materials and Fabrication

The controlled-composition steels used in this investigation were melted and fabricated in the laboratory. These steels, containing selected amounts of C, B, and Mn, were prepared by induction melting small 400 g heats in dry alumina crucibles and protected by a dry argon atmosphere. All boron additions were made using ferro-boron containing 17.88% B. Each ingot solidified unidirectionally to minimize piping. The resulting 1¼ in. diam × 3 in. ingots were annealed under a dry argon atmosphere and then cold rolled to ½ in. thick plate. The compositions of these steels are listed in Table 1.

Filler metal was also prepared from these induction melted ingots by cold rolling longitudinally cut sections of the ingots to ¼ in. diam bars. Stress relieving and spheroidizing heat treatments were performed as necessary to insure workability. The bars were swaged to a final diameter of 0.087 in. for use as weld filler metal.

In addition, several plain carbon and boron steels were commercially available. These steels were also rolled to ¼ in. thick plate and swaged to 0.087 in diam filler metal, as needed. The compositions of these steels are shown in Table 1.

Welding

All welding was performed by the gas tungsten-arc (GTA), gas metal-arc (GMA) and submerged arc processes. Bead-on-plate welds were deposited on ¼ in. thick plate specimens containing a U groove as shown in Fig. 2. Argon shielding gas (35cfh) was used to protect all GTA and GMA welds.

Metallography

Steel welds were sectioned longitudinally. These sections were electropolished in chromic acid solution and etched using: 1 ml HNO_3, 12 gm picric acid and 300 ml ethyl alcohol. Also, two-stage carbon replicas with chromium shadowing were prepared for electron microscopy.

Tensile Testing

Welded specimens were machined for tensile testing with and without notches as shown In Fig. 3. Unwelded notched and unnotched tensile specimens were also tested for reference. All tensile testing was performed at a strain rate of 0.1 ipm using the strain-controlled mode.

Weld Cooling Curves

Complete cooling curves of solidifying weld metal were obtained by immersion of a 0.010 in. diam 3% Re-W and 10% Re-W thermocouple into the molten weld pool. A continuous chart recorder plotted the resulting cooling curves.

Results and Discussion

Boron's Hardenability Effect in Weld Metal

Because there was no direct method of measuring the hardenability of as-deposited weld metal, a technique was devised whereby the hardenability of wrought steel (as determined by the Jominy end

quench test) could be compared with the hardenability of weld metal of the same composition. The known cooling rates associated with each 1/16 in. distance of the end quench test were matched with experimentally determined cooling rates of as-deposited GTA and GMA weld metal. The average weld metal hardness for each particular weld cooling rate as measured at 1300 F was compared to the hardness value obtained in the end quench test for the 1/16 in. distance corresponding to that same cooling rate.

For example, the hardenabilities of as-deposited 1020 and 10B20 steel weld metal were determined by comparison with standard end quench data (see Fig. 4) for 1020 and 10B20 wrought steels, respectively. Figure 5(a) and (b) show that, for a particular cooling rate, little or no difference existed between the average weld hardness and wrought metal hardness of the same steel. If, for example, the hardenability of 10B20 steel weld metal were significantly lower than the hardenability of 10B20 wrought steel, then the curve in Fig. 5(b) would have a slope less than 45 deg. But since the curve for the 10B20 steel had a slope of 45 deg, the hardenability of 10B20 steel weld metal was essentially the same as that of 10B20 wrought steel.

When comparing the hardenabilities of weld metal and wrought metal of the same composition, several sources of error must be accounted for. Most significant is the difference in austenite grain size and shape between weld and wrought products. In the weld metal and wrought metal tested in this work, there was fortunately little difference between the austenite grain size in the weld and in the corresponding wrought steel. Consequently, such a comparison between the hardenabilities of wrought and weld metal could be made.

Furthermore, the hardenability of boron steel weld metal was found to be greatly dependent upon the boron content of the weld. It is well known that too little or too much boron in a wrought steel (Ref. 1, 2, and 6) can diminish boron's hardenability effect. In this investigation, it was found that increasing the boron content beyond 0.0017% B progressively decreased boron's hardenability effect in as-deposited GTA and GMA welds (see Fig. 6). That is, excessive boron concentrations resulted in lower hardness weld metal for a particular weld cooling rate. However, it is important to note that despite the wide range of boron contents studied (0 to 0.024% B in Fig. 6), the boron-containing steel weld always had higher hardenability than the equivalent boron-free steel weld.

Boron's Effect on Weld Microstructure

The addition of boron had a considerable effect upon the microstructure of plain carbon steel weld metal, as-deposited by the GTA and GMA welding processes. It was evident that boron not only tended to form a borocarbide precipitate, $Fe_{23}(B,C)_6$, at prior austenite grain boundaries and solidification cell boundaries but also significantly altered the structure of the eutectoid transformation products during weld cooling.

A metallographic comparison was made on several identically welded 0.2% C steels containing different percentages of boron. Figures 7 through 10 show the microstructures of autogenous GTA weld metal made on 0.2% C steel containing no boron, 0.0017% B, 0.0082% B and 0.024% B, respectively. All welds were cooled at a rate of 70 F/s, measured at 1000 F. This corresponded to a heat input of approximately 300 A, 18 V and 12 ipm travel speed.

The microstructures of 1020 steel weld metal, deposited by the GTA process, are shown in Fig. 7. This boron-free weld was characterized by a coarse grain structure consisting of blocky and Widmanstatten ferrite, which outlined the prior austenite grain boundaries, Fig. 7(a). In Fig. 7(b), it was found that pearlite formed in areas which were adjacent to the blocky ferrite regions. Upper bainite, on the other hand, tended to form more toward the interior of the prior austenite grains. Such microstructures occur commonly in carbon steel welds.

Upon addition of 0.0017% boron to this 0.2% C steel weld, significant changes in weld microstructure occurred as shown in Fig. 8. Comparing Figs. 7(a) vs 8(a), it can be seen that boron promoted the precipitation of proeutectoid ferrite not only at

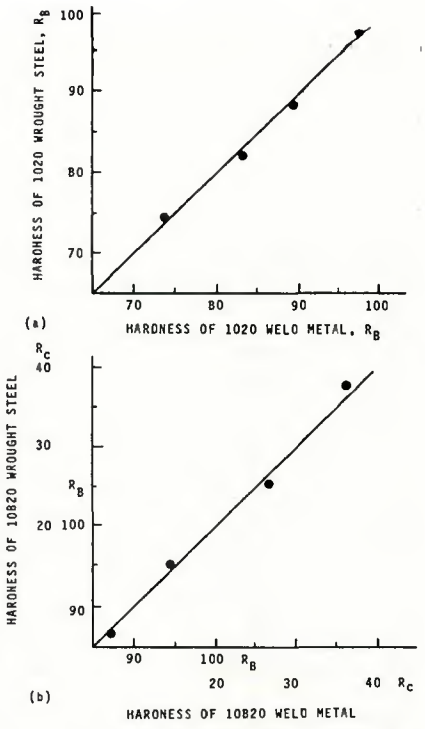

Fig. 5 — Comparison of hardness after equal cooling rates at 1300 F for wrought steel and weld metal of the same composition; (a) 1020 steel and (b) 10B20 steel

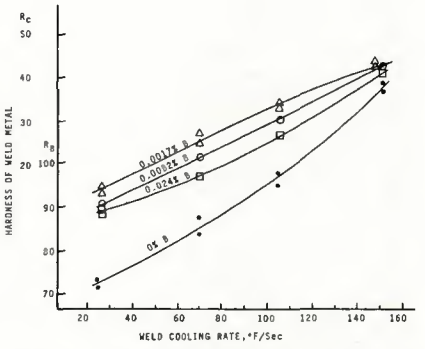

Fig. 6 — Effect of boron content and weld cooling rate at 1000 F on the hardness of 0.2% C steel welds

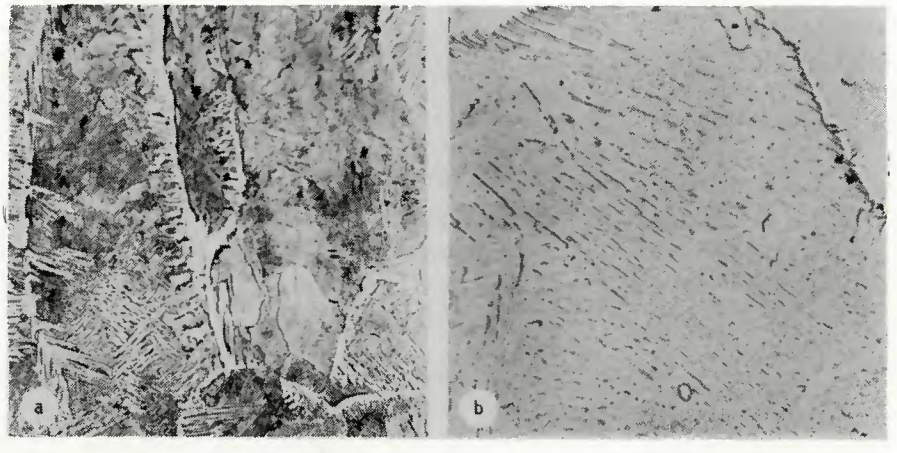

Fig. 7 — Microstructure of 1020 steel weld metal deposited by the GTA process. Weld cooling rate was 70 F/s at 1000 F. (a) X500 reduced 36.5% and (b) two-stage carbon replica, X6000, reduced 36.5%

prior austenite grain boundaries but also at solidification cell boundaries (reported in previous work, Ref. 7). The boron-free steel in Fig. 7(a) shows that proeutectoid ferrite formed only at prior austenite grain boundaries, and the cellular solidification substructure was not visible. That is, the cell boundaries were so weakly segregated with solute that they had essentially no effect upon the transformation products from austenite during weld cooling. However, the boron steel weld containing 0.0017% B, Fig. 8(a), shows that proeutectoid ferrite was precipitated at both cell boundaries and prior austenite grain boundaries. Here the solid state segregation of boron at cell as well as grain boundaries in austenite increased the strain energy of these boundary regions sufficiently to cause nucleation of proeutectoid ferrite at both cell and austenite grain boundaries during weld cooling. Consequently, the prior austenite grain and cell boundaries of the boron steel weld were nearly indistinguishable.

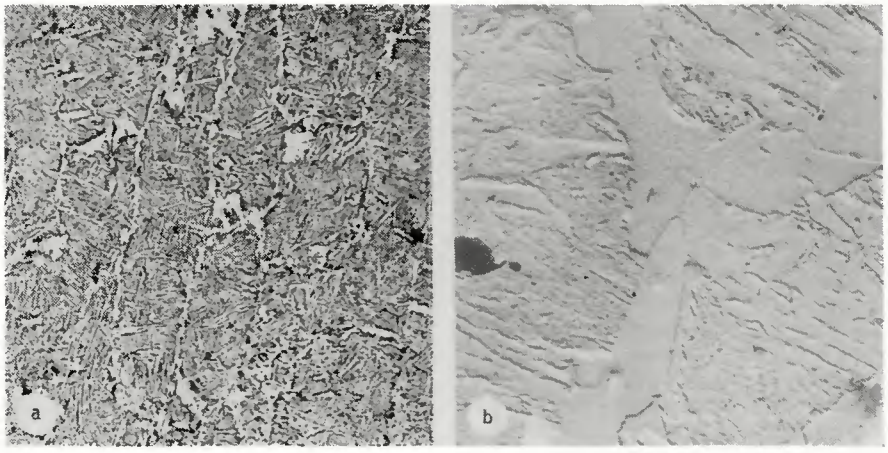

Fig. 8 — GTA weld metal of 10B20 steel containing 0.0017% boron. Weld cooling rate was 70 F/s at 1000 F. (a) X500 reduced 35% and (b) two-stage carbon replica, X6000, reduced 35%

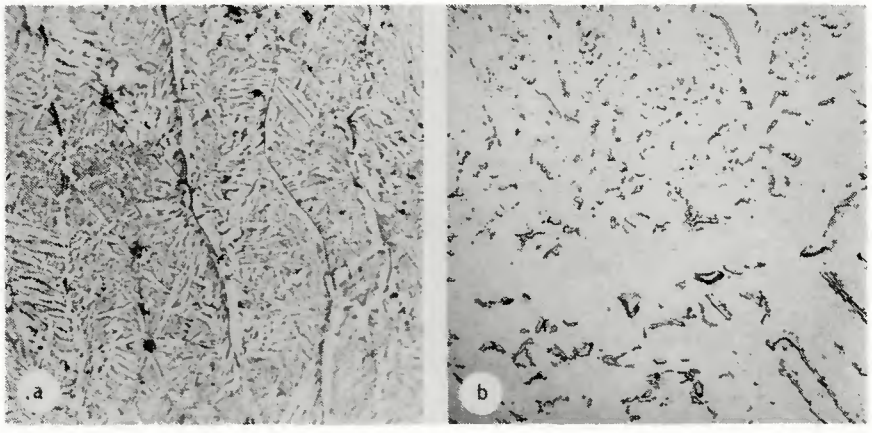

Fig. 9 — GTA weld metal of 0.2% C steel containing 0.0082% boron (sample B-3). Weld cooling rate was 70 F/s at 1000 F. (a) X600 reduced 30% and (b) two-stage carbon replica, X3000, reduced 30%

Furthermore, the addition of boron greatly suppressed the pearlite and upper bainite reactions. The boron addition promoted the formation of a ferrite-carbide aggregate in Fig. 8(b), which was quite similar in appearance to granular bainite (Ref. 9). Comparing Figs. 7(b) vs 8(b), it appeared that boron significantly altered the bainitic structure which formed upon weld cooling. In the microstructure of the 1020 steel weld metal in Fig. 7(b), upper bainite and small areas of pearlite were observed; while, the equivalent 10B20 steel weld containing 0.0017% B exhibited only a granular form of bainite without any trace of pearlite. It is well known that as little as 0.001 to 0.003% boron retards the pearlite transformation in steels. However, it is not well understood why boron so greatly affected the morphology of bainite in these steel welds. It is suspected that such behavior is undoubtedly related to boron's ability to alter the nucleation and growth mechanisms of bainitic structures.

Increasing the boron content of 0.2% C steel welds to 0.0082% and 0.024% B further enhanced the formation of this carbide-ferrite aggregate or granular bainite as shown in Figs. 9(b) and 10(c). These welds contained neither a trace of conventional pearlite nor upper bainite; instead, the microstructures show aci-

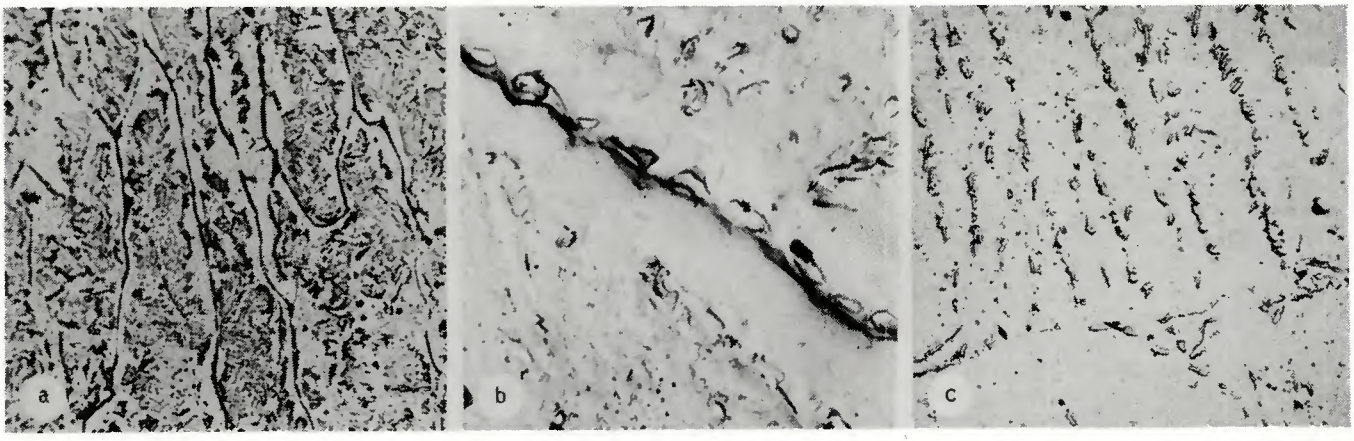

Fig. 10 — GTA weld metal of 0.2% C steel containing 0.024% boron (sample B-4). Weld cooling rate was 70 F/s at 1000 F. (a) X500, reduced 23.5%, (b) and (c) two-stage carbon replicas, X6000, reduced 23.5%

cular and nodular arrays of carbide in a ferrite matrix which correspond in appearance to the nodular and acicular formations of granular bainite. This structure was particularly prominent with increasing boron content as can be seen by comparing Figs. 8 through 10.

Borocarbide Precipitation in Welds

The boron content of steel weld metal was found to greatly affect the amount of borocarbide precipitation occurring at both solidification cell boundaries and austenite grain boundaries during cooling of GTA and GMA welds. Figures 7 through 10 show this intergranular and intercellular precipitation in 0.2% C steel welds as a function of boron content for a weld cooling rate of 70 F/s, measured at 1000 F. The GTA weld microstructure of the 1020 steel (boron-free) in Fig. 7, of course, contained no borocarbides in boundary regions. Indeed, the 0.2% C steel weld containing 0.0017% boron in Fig. 8 contained only traces of borocarbide constitutent at boundary areas for this 70 F/s weld cooling rate.

However, with further increases in boron content to 0.0082% B (Fig. 9), the borocarbide precipitation became prominant. Finally, when an excessive amount of boron (0.024% B) was added to 0.2% C steel weld metal, a preponderance of intergranular and intercellular borocarbide precipitation occurred as shown in Fig. 10. The borocarbide phase precipated as fine "dots", which appeared quite evenly distributed along both cell and prior austenite grain boundaries.

The intergranular and intercellular borocarbide in Figs. 8, 9, and 10 always appeared to form in a matrix of proeutectoid ferrite, which also outlined the prior austenite grain and cell boundaries. This was due to boron's strong tendency to segregate by interstitial diffusion to austenite grain and cell boundaries during weld cooling. When the boron concentrations at the boundaries became supersaturated, the elastic strain energy of the boundary increased up to the point where borocarbide precipitation occurred. Simultaneously, these regions of high strain energy also served as active nucleating sites for proeutectoid ferrite. Consequently, when weld cooling rates for 0.2% C boron steels were about 70 F/s or less, both borocarbides and proeutectoid ferrite precipitated. Both phases formed along prior austenite grain and cell boundaries but the borocarbide phase precipitated as a linear array of "dots" in a "white" proeutectoid ferrite background as typically illustrated in Fig. 10(b).

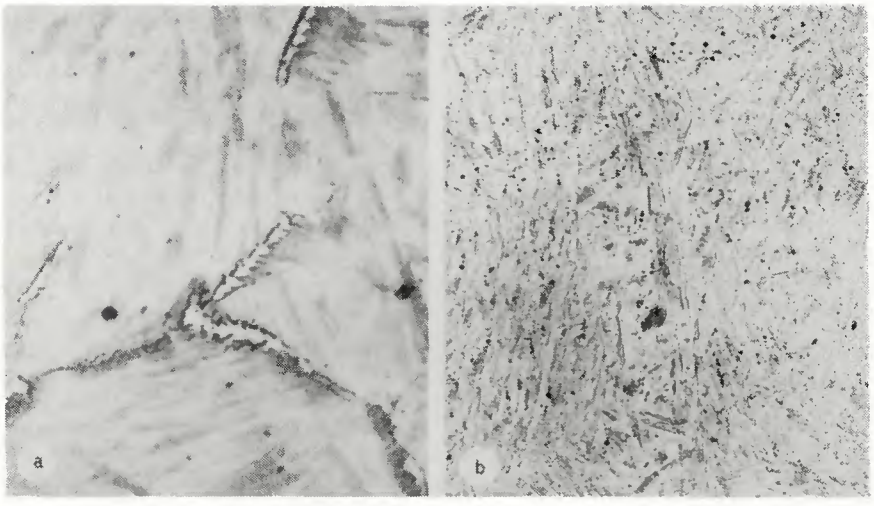

Fig. 11 — GTA weld metal of (a) 1020 steel, X2500, reduced 34% and (b) 10B20 boron steel, X600, reduced 34%. Both welds cooled at 150 F/s at 1000 F

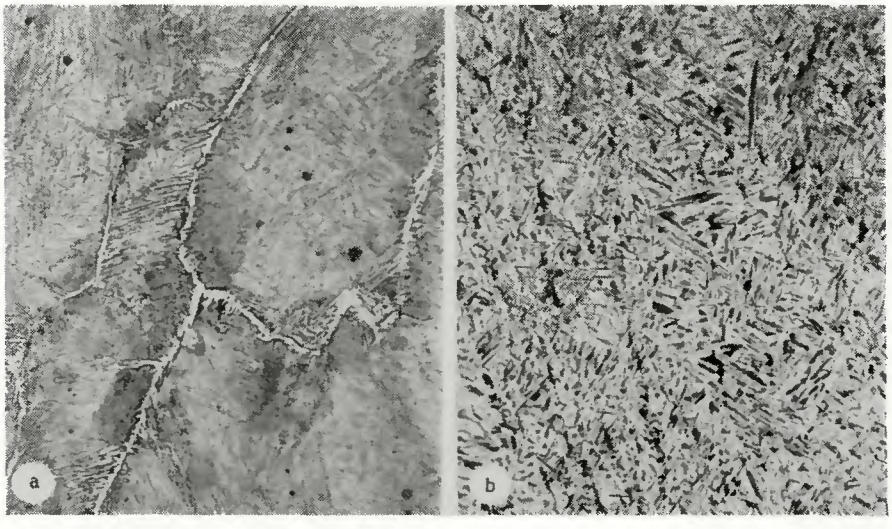

Fig. 12 — GTA weld metal of (a) 1020 steel and (b) 10B20 boron steel cooled at 105 F/s 1000 F. X600, reduced 32%

Effect of Cooling Rate on Weld Microstructure

With the exception of composition, weld cooling rate was the most significant factor affecting weld metal microstructures. As with plain carbon steel welds, the ability of boron steel weld metal to produce martensite during cooling was strongly dependent upon weld cooling rate. Since 0.0017% boron was found to increase the hardenability of 0.2% C steel weld metal by a factor of 2, the boron steels in Figs. 11 and 12 clearly contained more martensite than the corresponding boron-free steel weld. In Fig. 11 the boron steel weld fusion zone contained 100% martensite when cooled at 150 F/s (measured at 1000 F) while the boron-free steel contained small patches of proeutectoid ferrite and acicular upper bainite in a matrix of martensite.

Similarly in Figure 12(b) where the weld cooling rate was lowered to 105 F/s, the boron steel weld again contained a majority of martensite with only traces of Widmanstätten ferrite and upper bainite. The corresponding boron-free steel weld in Fig. 12(a) displayed lower hardenability with a microstructure containing large amounts of blocky and Widmanstätten ferrite, bainite and only small portions of martensite. It was metallographically evident that the ability of boron steel welds to produce martensite upon cooling was greater than similar steel welds without boron.

Effect of Cooling Rate on Borocarbide Precipitation

The cooling rate of GTA and GMA welds had a significant effect upon the amount of borocarbide precipitation occurring at austenite grain and cell boundaries. For a particular boron

content, slow weld cooling rates promoted extensive intergranular and intercellular precipitation while faster cooling rates tended to retard such precipitation.

GTA and GMA welds made on 10B20 steel with 10B20 filler metal became more prone to intergranular and intercellular precipitation as the cooling rate of the weld was decreased as shown in Fig. 13. The data in Fig. 13 is based on a comparison with the amount of borocarbide obtained by the Grange test (Ref. 3).

The large amount of borocarbide precipitation obtained by the Grange test (in Fig. 14) was arbitrarily taken to be 10 on a scale from zero (no borocarbides observed) to 10 (maximum amount of intergranular borocarbides). Figure 13 clearly showed that borocarbide formation increased significantly with decreasing weld cooling rates. Of course, the amount of precipitation was also contingent upon the initial boron content of the steel weld. That is, with increasing boron content, the curve in Fig. 13 would be shifted upward; while, for lower boron contents this curve would be shifted downward.

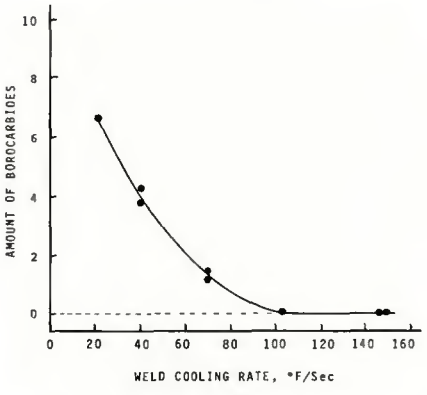

Fig. 13 — Effect of weld cooling rate (measured at 1000 F) on the relative amount of intergranular and intercellular borocarbide precipitation occurring in 10B20 steel weld metal containing 0.0017% boron

Nucleation of Proeutectoid Ferrite and Borocarbide

Although proeutectoid ferrite and borocarbide nucleation was affected by weld cooling rate, the austenite grain boundaries were found to be far more potent nucleating sites for proeutectoid ferrite and borocarbide precipitation than solidification cell boundaries. For example, when the weld cooling rate of 0.2% C boron steel welds was excessively fast, no proeutectoid ferrite occured, Fig. 11(b). Conversely, when slower cooling rates were used, proeutectoid ferrite occurred at both austenite grain and cell boundaries (Figs. 8, 9 and 10).

However, at an intermediate cooling rate at 105 F/s (at 1000 F), the austenite grain boundaries shown in Figs. 15(a) and (b) clearly precipitate proeutectoid ferrite while the cell boundaries were free of ferrite. The electron micrograph in Fig. 16 shows a ferrite-free cell boundary delineated by a fine borocarbide precipitate. In addition, the amount of borocarbide precipitation at grain boundaries was much greater than that occurring at solidification cell boundaries.

The explanation of this phenomenon undoubtedly is related to the fact that the austenite grain boundary was a high angle boundary with high elastic strain energy associated with this region; while, the cell boundary was a lower energy region equivalent to subgrain or tilt boundaries. Although the cellular segregation of substitutional solute atoms was about the same at both grain boundaries and cell boundaries (Ref. 7), the higher energy grain boundaries were the more likely sites for solid state segregation of the oversized interstitial boron atoms in austenite during weld cooling.

Because the boundaries represented areas of large elastic strain energy due to atomic mismatch, the diffusion and segregation of boron to high energy boundaries in austenite served to reduce the energy of the boundary. However, when the boundary became supersaturated with boron, the elastic strain energy of that boundary again increased until the boundary became an active nucleating site for both proeutectoid ferrite and borocarbide constituent.

Since the prior austenite grain boundary in welds, Fig. 16(a) and (b), represented a higher energy region than the cell boundary, the amount of boron segregation at the grain boundary would be proportionally greater than that at the cell boundary. Consequently, subsequent precipitation of proeutectoid ferrite and borocarbides was more abundant at the grain boundaries than at lower energy cell boundaries.

Transfer of Boron Across the Arc

The transferability of boron across the welding arc for the GTA, GMA and

Fig. 14 — Intergranular borocarbides resulting from heat treating 10B20 steel weld metal to 2000 F for 15 minutes, then quenching to 1200 F for 10 minutes. X1000, reduced 28%

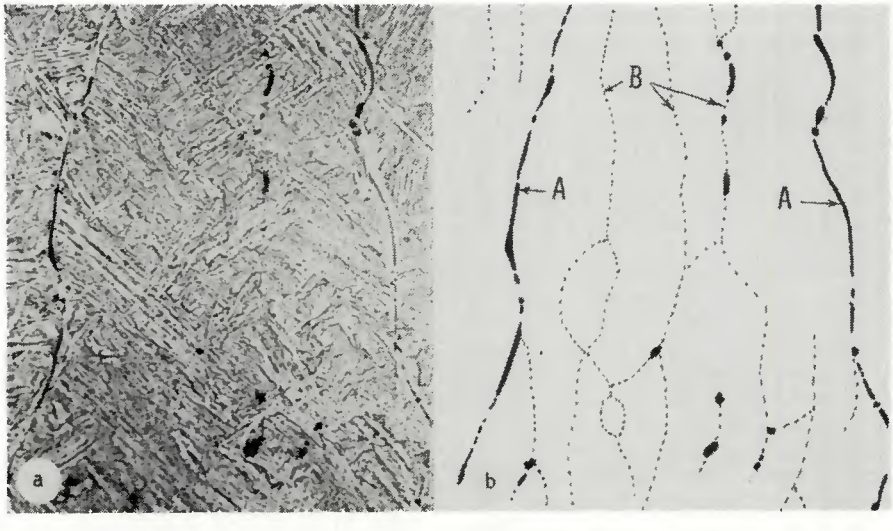

Fig. 15 — GTA weld metal of 0.2% C steel containing 0.024% boron. (a) Weld microstructure cooled at 105 F/s and (b) schematic representation of microstructure in (a) showing: region "A" = prior austenite grain boundaries which have nucleated both borocarbides and proeutectoid ferrite; and region "B" = cell boundaries containing borocarbides only. X600, reduced 28%

submerged arc welding processes was determined but only for those relatively low weld heat inputs used in this investigation. Multipass welds were deposited on 1020 steel plate with 10B20 filler metal using approximately 300 A and 20 V for each welding process.

It was found that most of the boron contained in the filler metal transferred successfully across the welding arc into the weld pool. From Table 2, virtually no boron was lost through the arc in the submerged arc process; while, the GTA and GMA processes suffered minor losses of boron during transfer through the arc for the welding parameters used in this investigation.

Effect of Boron on Notch Tensile Strength

Boron content was found to have a substantial effect upon the notch sensitivity and notched tensile strength of carbon steel weld metal, as-deposited by the GTA and GMA processes. There existed an optimum range of boron concentrations over which the maximum notched tensile strength occurred. Lower than the optimum boron content resulted in lower notched tensile strength; while, excessive amounts of boron caused the welds to become notch sensitive due to the precipitation of intergranular and intercellular borocarbides.

To illustrate this, several GTA and GMA welds were deposited on 2020 and 10B20 steel plate in a manner shown in Fig. 2 using filler metal of essentially the same composition as the plate stock except for its boron content. All welds were deposited at 300 A, 20 V and 12 ipm travel speed resulting in a weld cooling rate of 70 F/s, measured at 1000 F. The notch tensile strength of these GTA welds was found to be extremely dependent upon boron content as shown in Fig. 17. Clearly, there was an optimum range of boron content which resulted in maximum notch tensile strength (for a particular weld composition and cooling rate).

For the GTA welds deposited on 10B20 boron steel shown in Fig. 17, the optimum range of boron content resulting in maximum notched tensile strength was about 0.001 to 0.003% B. The welds deposited on 1020 steel (boron-free) were limited to 0.0017 to 0.003% B. Similar results were obtained when GMA welds were tested. The data in Fig. 17 is in general agreement with work by Melloy et al (Ref. 6) on wrought boron steels where boron's effect on the strength and hardenability of steel was maximized at 0.0026% B.

In addition, as the weld boron content exceeded about 0.003% B, the amount of $Fe_{23}(B,C)_6$ borocarbides precipitating at boundaries increased. These borocarbides, being incoherent with its matrix, greatly weakened the grain and cell boundaries of GTA and GMA weld metal. Thus, after notch tensile testing, it was found that excessive boron concentrations tended to promote intergranular and intercellular fractures similar to the "rock-candy" type of fracture.

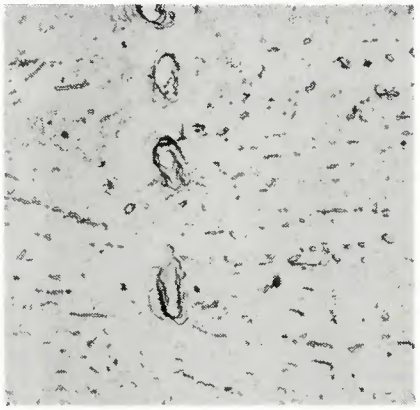

Fig. 16 — Two-stage carbon replica showing the cell boundary precipitation of borocarbides in region "B" of Figure 15(b). X6000, reduced 28%

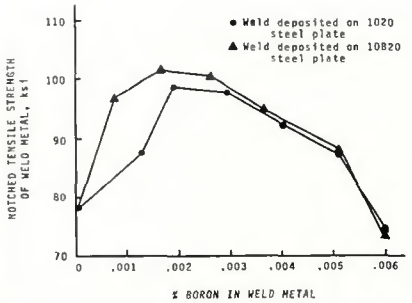

Fig. 17 — Effect of boron content on the notched tensile strength of 0.2% C steel weld metal deposited by the GTA process

Table 2 — Transferability of Boron Across the Welding Arc

Welding process	No. of Passes	Boron, %	% Transferred
Sub arc	5[a]	0.0015	100
GTA	6[a]	0.0014	93
GMA	6[a]	0.0013	87
Filler metal (reference)	—	0.0015	—

(a) Actual analysis was performed on the last pass of weld

Effectiveness of Boron Transferred Across the Arc

It was found that the effectiveness of boron in GTA, GMA and submerged arc weld metal was significantly influenced by whether the boron entering the weld came from the filler metal (i.e., transferred across the arc) or from the base metal. Upon examining Fig. 17, it was clear that in steel welds containing less than about 0.002% boron, the effect of boron upon increasing the weld notch tensile strength was greater in welds where the boron entered the weld fusion zone by base metal dilution (i.e., boron-free filler metal deposited on 10B20 boron steel plate) than in welds where the boron had entered the weld solely by transfer across the arc (i.e., boron steel filler metal deposited on boron-free 1020 steel). Even so, much stronger welds were obtained when boron steel filler metal was used to weld boron-free plate.

Furthermore, this phenomenon appeared to be related to the amount of "soluble" boron present in the weld. Chemical analysis has shown that for welds containing less than 0.002% total boron, the amount of soluble boron in the welds deposited on the 10B20 boron steel plate was greater than that in the welds made on 1020 steel plate, where all the boron in the weld was transferred across the arc. Consequently, even though the total boron content of the welds was the same, the welds containing boron from base metal dilution possessed a significantly higher percentage of "soluble" boron than those welds which gained boron solely by transfer across the welding arc (compare curves in Fig. 17 for % B < 0.002%).

To verify this effect, GTA, GMA and submerged arc welds were deposited on 1020 and 10B20 steel plates using filler metal made from these same steels. Figure 18 shows the notched tensile strengths of welds made by depositing (a) 1020 steel filler metal on 1020 plate, (b) 1020 filler on 10B20 plate, (c) 10B20 filler on 1020 plate and (d) 10B20 filler on 10B20 plate. Clearly, the welds depoisited on the 10B20 boron steel plate resulted in the highest notched tensile strength. The welds containing no boron at all had the lowest strength; but, the welds of 10B20 filler metal on 1020 steel plate had an intermediate strength level.

A chemical analysis of these welds in Fig. 18 further revealed that significantly more soluble boron was transmitted to the weld pool by base metal dilution than by transfer across the welding arc even though the total amount of boron entering the weld might have been the same. Consequently, when the notched tensile data were plotted as a function of soluble boron content of the weld fusion zone, it was found that the notched tensile strength increased with increasing soluble boron content as

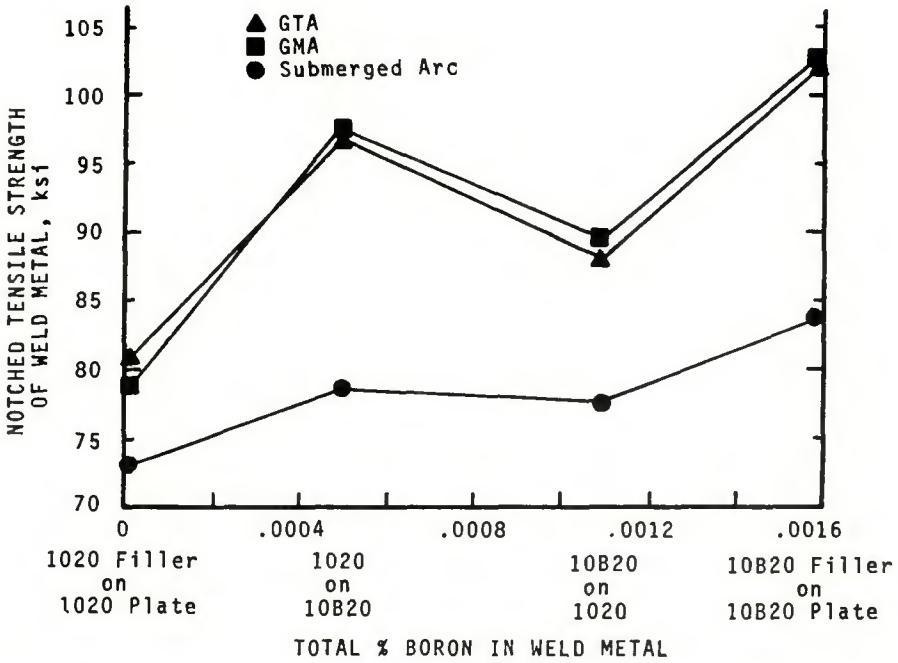

Fig. 18 — Effect of boron on the notched tensile strength of steel weld metal deposited by the GTA, GMA and submerged arc processes using 300 A, 20 V and 12 ipm travel speed

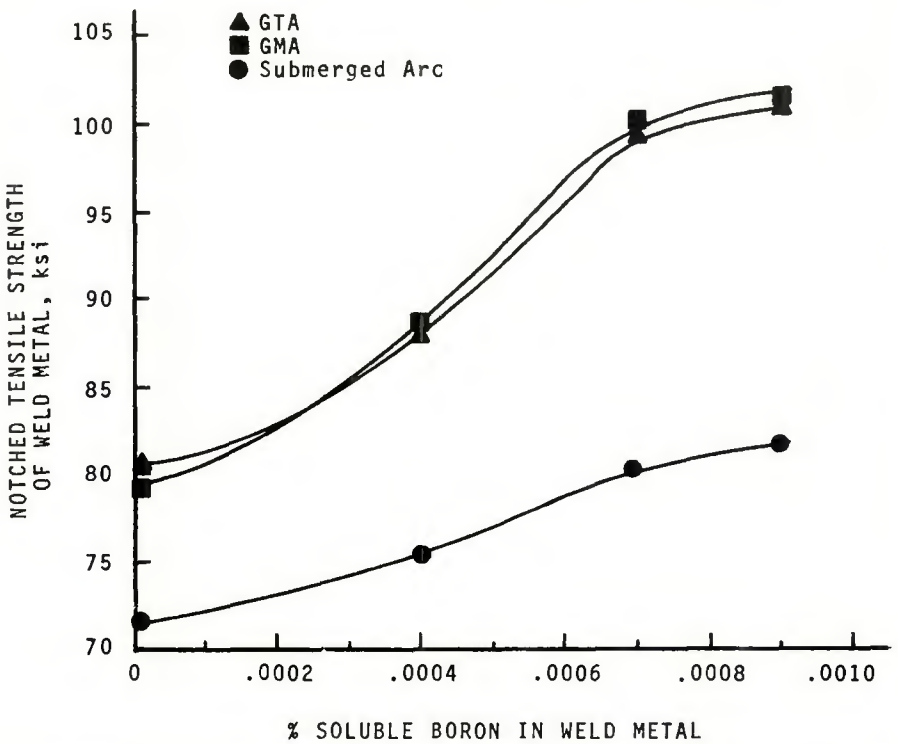

Fig. 19 — Effect of "soluble" boron content on the notched tensile strength of 0.2% C steel weld metal

shown in Fig. 19.

Why boron transferred across the arc is not as effective a transmitter of soluble boron as boron gained by base metal dilution is not well understood. However, recent work by Margrave et al (Ref. 20) has shown several elements including boron could form compounds when exposed to extremely high temperature in the presence of other elements. Although the temperature of the welding arc is more than 10,000 F, the filler metal melt-off rate is fast enough that the soluble boron in the filler metal is not exposed to these elevated temperatures for more than a fraction of a second during the transfer across the arc. Consequently, if soluble boron were combining with some other element in the arc, only a small proportion of the soluble boron would probably be lost. This mechanism could explain boron's decreased effectiveness upon transferring across the arc (Fig. 17), but there is no direct experimental evidence under welding conditions to support the hypothesis.

On the basis of the data presented in this investigation, boron could be beneficially utilized for commercial welding applications. When boron steel plates are welded with boron steel filler metal, boron's hardenability effect has been shown to be equally potent in steel weld metal as it is in wrought steel of the same chemical composition (Figs. 5 and 6). Furthermore, the use of boron steel filler metal to weld boron steels as well as plain carbon steels has been shown to substantially increase the notched tensile strength of the weld. Such increases in weld strength occur most significantly in GTA, GMA welds and to a lesser extent in the slow cooling submerged arc welds (Figs. 17, 18 and 19). Since as little as 0.002% to 0.003% boron has the same hardenability factor as much larger quantities of expensive alloying elements in steel such as Ni or Mo, the cost savings should be a significant factor in future selection of filler metal for welding boron and carbon steels.

Conclusions

Boron was found to have the following effects upon the microstructure, hardenability and notched tensile properties of steel welds, as-deposited by the GTA and GMA welding processes.

1. Boron retards the formation of pearlite and upper bainite and promotes a structure similar in appearance to granular bainite.

2. The amount of $Fe_{23}(B,C)_6$ borocarbide forming at austenite grain boundaries and solidification cell boundaries increases with (a) increasing boron content in the weld and (b) decreasing weld cooling rate.

3. The austenite grain boundaries are slightly more potent nucleating sites for the precipitation of proeutectoid ferrite than solidification cell boundaries during weld cooling.

4. Boron's hardenability factor in as-deposited steel weld metal is essentially the same as that in wrought steel of the same composition. The hardenability factor for boron in 10B20 wrought steel and GTA and GMA weld metal was 2.0.

5. The notched tensile strength of boron steel weld metal is dependent upon boron content. There is an optimum boron content of approximately 0.002% which corresponds to maximum notched strength. The reduction of notched strength at excessive boron concentrations is due to the presence of intergranular and

intercellular borocarbides.

6. The notched tensile strength of GTA, GMA and also submerged arc welds varied directly as a function of the "soluble" boron content of the weld rather than the total spectrographic boron concentration.

7. Virtually all the boron in steel filler metal is transferred across the arc for the GTA, GMA and submerged arc processes provided the welding parameters are less than approximately 300 A, 20 V and 12 ipm travel speed.

8. The notched tensile strength of boron steel welds deposited by the GTA and GMA processes was generally greater than those deposited by the submerged arc process.

9. Filler metal containing boron produces consistently stronger welds than boron-free filler welds regardless of whether the base metal is plain carbon or boron steel.

References

1. Simcoe, C. R., Elsea, A. R. and Manning, G. K., "Study of Boron on the Decomposition of Austenite", *Transactions AIME*, 203, 1955, pp 193-200.

2. Grange, J.A. and Mitchell, J. B., "On the Hardenability Effect of Boron in Steel", *Transactions ASM*, 53, 1961, pp 157-180.

3. Grange, R. A. and Garvey, T. M., "Factors Influencing the Hardenability of Boron-Treated Steels", *Transactions ASM*, 37, 1946, pp 136-192.

4. Crafts, W. and Lamont, J. L., "Effect of Some Elements on Hardenability", *Transactions AIME*, 158, 1944, pp 157-167.

5. Udy, M. C. and Rosenthal, P. C., "Boron in Certain Alloy Steels", *Transaction AIME*, 172, 1947, pp 273-302.

6. Melloy, G. F., Slimmon, P. R. and Pidgursky, P. D., "Optimizing the Boron Effect", *Met. Transactions*, 4, 1973, pp 2279-2289.

7. Devletian, J. H. and Heine, R. W., "Grain Refining Effect of Boron in Carbon Steel Welds", *Welding Journal*, Vol. 52 (12), Dec. 1973, Res. Suppl., pp 529-s to 535-s.

8. Rahrer, G. D. and Armstrong, C. D., "The Effect of Carbon Content on the Hardenability of Boron Steels", *Transactions ASM*, 40, 1948, pp 1099-1123.

9. Schrader, A. and Rose, A., *De Ferri Metallographia*, Vol. II, Verlag Stahleisen MBH, Dusseldorf, W. Germany, 1966, pp 342-348.

10. Margrave, J. L. and Mamontov, G., *High Temperature Materials and Technology*, Wiley, New York, 1967, pp 78-127.

WRC Bulletin No. 198
SEPT. 1974

"Secondary Stress Indices for Integral Structural Attachments to Straight Pipe"

by W. G. Dodge

"Stress Indices at Lug Supports on Piping Systems"

by E. C. Rodabaugh, W. D. Dodge and S. E. Moore

This report presents a simplified method for calculating the stresses induced in straight pipe by thrust and moment loadings applied to lugs and other integral attachments. Following the philosophy of the nuclear power piping portion of Section III of the ASME Boiler and Pressure Vessel Code, appropriate secondary stress indices are defined. A simple and conservative formula for computing the stress indices is developed using analytical results as a guide. A comparison is made between experimental stress indices and those obtained using the simplified analysis procedure developed here as well as the more complex analysis procedures of *Welding Research Council Bulletin 107* (WRC-107 method). The method is extended to attachments having a variety of cross sections.

Stress indices and the appropriate simplified design formulas are developed for analyzing integral lug attachments on straight pipe according to the philosophy of Section III of the ASME Boiler and Pressure Vessel Code for Class I Piping Systems. Indices are developed for the evaluation of primary stresses, primary-plus-secondary stresses, and peak stresses due to internal pressure in the pipe for radial thrust and transverse shear forces and torsional and bending moment loads acting on the lug; and for a thermal gradient between the pipe and the lug. The indices for thrust and bending moment loads are based on an extensive parameter study and are represented by simple formulas that may be used directly by designers and/or incorporated into codes and standards. From comparisons with other methods of analysis these formulas are considered to be more accurate and easier to use. Indices for the other loadings are based in part on strength-of-materials theory and information in the literature. Specific recommendations are made for incorporating the stress indices and design formulas into the ASME Code. As an example, a simple pipe support design is analyzed using the recommended formulas.

Publication of these papers was sponsored by the Pressure Vessel Research Committee of the Welding Research Council. The price of WRC Bulletin 198 is $6.00. Orders should be sent to the Welding Research Council, 345 East 47th Street, New York, N.Y. 10017.